The Journal of Immunology

RESEARCH ARTICLE | JUNE 15 2015

Determinants of Gliadin-Specific T Cell Selection in Celiac Disease

Jan Petersen; ... et. al

J Immunol (2015) 194 (12): 6112–6122.
https://doi.org/10.4049/jimmunol.1500161

Determinants of Gliadin-Specific T Cell Selection in Celiac Disease

Jan Petersen,*,†,[1] Jeroen van Bergen,‡,[1] Khai Lee Loh,* Yvonne Kooy-Winkelaar,‡ Dennis X. Beringer,* Allan Thompson,‡ Sjoerd F. Bakker,§ Chris J. J. Mulder,§ Kristin Ladell,¶ James E. McLaren,¶ David A. Price,¶,‖ Jamie Rossjohn,*,†,¶,[2] Hugh H. Reid,*,[2] and Frits Koning‡,[2]

In *HLA-DQ8*–associated celiac disease (CD), the pathogenic T cell response is directed toward an immunodominant α-gliadin–derived peptide (DQ8-glia-α1). However, our knowledge of TCR gene usage within the primary intestinal tissue of *HLA-DQ8*$^+$ CD patients is limited. We identified two populations of HLA-DQ8-glia-α1 tetramer$^+$ CD4$^+$ T cells that were essentially undetectable in biopsy samples from patients on a gluten-free diet but expanded rapidly and specifically after antigenic stimulation. Distinguished by expression of TRBV9, both T cell populations displayed biased clonotypic repertoires and reacted similarly against HLA-DQ8-glia-α1. In particular, TRBV9 paired most often with TRAV26-2, whereas the majority of TRBV9$^-$ TCRs used TRBV6-1 with no clear *TRAV* gene preference. Strikingly, both tetramer$^+$/TRBV9$^+$ and tetramer$^+$/TRBV9$^-$ T cells possessed a non–germline-encoded arginine residue in their CDR3α and CDR3β loops, respectively. Comparison of the crystal structures of three TRBV9$^+$ TCRs and a TRBV9$^-$ TCR revealed that, as a result of distinct TCR docking modes, the HLA-DQ8-glia-α1 contacts mediated by the CDR3-encoded arginine were almost identical between TRBV9$^+$ and TRBV9$^-$ TCRs. In all cases, this interaction centered on two hydrogen bonds with a specific serine residue in the bound peptide. Replacement of serine with alanine at this position abrogated TRBV9$^+$ and TRBV9$^-$ clonal T cell proliferation in response to HLA-DQ8-glia-α1. Gluten-specific memory CD4$^+$ T cells with structurally and functionally conserved TCRs therefore predominate in the disease-affected tissue of patients with HLA-DQ8–mediated CD. ***The Journal of Immunology*****, 2015, 194: 6112–6122.**

The genetic and mechanistic bases of type I diabetes, rheumatoid arthritis, and celiac disease (CD) show considerable overlap in terms of distinct associations with autoantibodies, particular *HLA class II* alleles, and posttranslationally modified T cell epitopes (1). These features indicate that HLA class II–restricted CD4$^+$ T cells play a pivotal role in the etiology of these diseases. It is therefore important to track and characterize the relevant Ag-specific T cells in patients as a prelude to novel prophylactic or therapeutic interventions.

CD is a disease of the small intestine caused by intolerance to dietary gluten, a family of gliadin and glutenin proteins present in the commonly consumed cereals wheat, barley, and rye (1). In CD patients, crypt cell hyperplasia and villous atrophy in the duodenum impair nutrient absorption from food, leading to some of the typical symptoms associated with the disease: diarrhea, growth retardation in children, and osteoporosis. CD is common, affecting ≤1% of the white population (2). It is strongly associated with the presence of *HLA-DQA* and *HLA-DQB* alleles encoding HLA-DQ2 (*DQA1*0501-DQB1*0201*) and HLA-DQ8 (*DQA1*0301-DQB1*0302*) in ∼95% and 5% of CD patients, respectively (3). These associations are explained by the observation that CD4$^+$ T cells specific for gluten-derived peptides bound to either HLA-DQ2 or HLA-DQ8 are found in small-intestinal biopsy specimens from patients but not controls (1, 2, 4). Typically, in HLA-DQ2–associated disease, the immunodominant gluten epitopes are derived from proline-rich, degradation-resistant regions of the gliadin proteins in which certain glutamine residues are deamidated to glutamic acid via the activity of the enzyme tissue transglutaminase (TG2) (5–7). Many studies have shown that this selective deamidation is required for efficient binding of gliadin peptides to HLA-DQ2 (5, 7). In contrast, the immunodominant gliadin epitope in HLA-DQ8–mediated disease is derived from a protease-sensitive region, and T cell responses to both the native gliadin peptide and deamidated variants have been observed (7, 8).

*Department of Biochemistry and Molecular Biology, School of Biomedical Sciences, Monash University, Clayton, Victoria 3800, Australia; †Australian Research Council Centre of Excellence in Advanced Molecular Imaging, Monash University, Clayton, Victoria 3800, Australia; ‡Department of Immunohematology and Blood Transfusion, Leiden University Medical Center, Leiden 2333 ZA, the Netherlands; §Department of Gastroenterology, Free University Medical Center, Amsterdam 1081 HZ, the Netherlands; ¶Institute of Infection and Immunity, Cardiff University School of Medicine, Heath Park, Cardiff CF14 4XN, United Kingdom; and ‖Vaccine Research Center, National Institute of Allergy and Infectious Diseases, National Institutes of Health, Bethesda, MD 20892

[1]J.P. and J.v.B. contributed equally to this work.

[2]J.R., H.H.R., and F.K. contributed equally to this work.

Received for publication January 23, 2015. Accepted for publication April 4, 2015.

This work was supported by the Australian Research Council, the National Health and Medical Research Council of Australia (No. 1085875), the Celiac Disease Consortium, an Innovative Cluster approved by the Netherlands Genomics Initiative and supported by the Dutch government (No. BSIK03009), and the Wellcome Trust. J.R. is supported by an Australia Fellowship from the National Health and Medical Research Council. D.A.P. is supported by a Wellcome Trust Senior Investigator Award.

The coordinates and structure factors presented in this article have been submitted to the Protein Data Bank (http://www.wwpdb.org/) under entry codes 4Z7U, 4Z7V, and 4Z7W.

Address correspondence and reprint requests to Prof. Jamie Rossjohn and Dr. Hugh H. Reid or Prof. Frits Koning, Department of Biochemistry and Molecular Biology, School of Biomedical Sciences, Monash University, Clayton, VIC 3800, Australia (J.R. and H.H.R.) or Department of Immunohematology and Blood Transfusion, Leiden University Medical Center, Leiden 2333 ZA, the Netherlands (F.K.). E-mail addresses: jamie.rossjohn@monash.edu (J.R.) and hugh.reid@monash.edu (H.H.R.) or F.Koning@lumc.nl (F.K.)

The online version of this article contains supplemental material.

Abbreviations used in this article: BSA, buried surface area; CD, celiac disease; p, position; PEG, polyethylene glycol; TG2, transglutaminase; vdw, van der Waals'.

Although the potential TCR repertoire in humans is vast, several recent reports have demonstrated that immunodominant gliadin epitopes elicit heavily biased responses. In particular, T cells specific for the DQ2.5-glia-α2 peptide preferentially express TRBV7-2, whereas those specific for DQ8-glia-α1 typically use TRBV9 (9–12). Such observations generally reflect structural and/or recombinatorial constraints (13, 14). Indeed, the first insights into the molecular basis for this biased TRBV usage have been obtained via crystallographic studies (9, 10).

A single crystal structure of a TRBV9$^+$ TCR-HLA-DQ8-glia-α1 complex shows that two amino acid residues virtually unique to TRBV9 are essential for TCR binding to the HLA-DQ8-glia-α1 complex, thereby providing a potential explanation for TRBV9 bias in HLA-DQ8–mediated CD (9). However, the observed bias toward TRBV9 does not necessarily extend to the affected intestinal tissue of patients because the HLA-DQ8–restricted T cells examined in this study were derived from long-term biopsy cultures. To obtain a more physiological picture of the HLA-DQ8-glia-α1–specific TCR repertoire in CD patients, we used tetrameric Ag complexes to isolate, clone, and characterize HLA-DQ8-glia-α1–specific T cells from small-intestinal biopsy material. In addition, we determined the ternary structures of two TRBV9$^+$ TCR-HLA-DQ8-glia-α1 and one TRBV9$^-$ TCR-HLA-DQ8-glia-α1 complex, thereby revealing the molecular interactions underlying HLA-DQ8–mediated CD.

Materials and Methods

Patients

The study was approved by the Medical Ethics Committees of the Free University Medical Centre and the Leiden University Medical Center. Written informed consent was obtained from each subject before enrollment. Patients S, T, vL, LS, and SP have been described previously (9, 15). Additional HLA class II genotypes were as follows: patient E, *HLA-DQA1*0301-DQB1*0302* homozygous; patient B, *HLA-DQA1*0301-DQB1*0302* homozygous; patient Bel, *HLA-DQA1*03/03-DQB1*0301/0302* heterozygous; patient C, *HLA-DQA1*0101/0301-DQB1*0501/0302* heterozygous. All patients were *HLA-DQ8*$^+$.

Ags and peptides

Preparation of a pepsin/trypsin digest of gluten, tissue TG2 treatment, and peptide synthesis were performed as described previously (7).

Gluten-specific T cell lines

To generate polyclonal gluten-specific T cell lines from the small intestine of CD patients, biopsy specimens were cultured with a TG2-treated gluten digest for 5 d, then expanded via the addition of IL-2 (20 Cetus units/ml; Novartis) and IL-15 (10 ng/ml; R&D Systems). The resulting T cell lines were stored in liquid nitrogen.

Tetramer-based isolation of T cell clones

Cells were released from small-intestinal biopsy specimens by incubation for 60 min with collagenase type IV (Worthington) at a concentration of 10 U/ml in a total volume of 3 ml. The isolated cells or short-term cultures were labeled with PE-conjugated tetramer for 60 min at 37°C, then stained with αTRBV9-FITC (Beckman Coulter) and αCD4-APC (BD Biosciences) for 30 min at 37°C. Tetramer$^+$ CD4$^+$ T cells were sorted for downstream culture using a FACSAria flow cytometer (BD Biosciences).

T cell proliferation assays

Proliferation assays were performed as described previously (15). A 13mer version of the DQ8-glia-α1 epitope (sequence SG**EGSFQPSQE**NP; amino acid core in bold) and variants with single alanine or glutamic acid substitutions were used as Ags.

Isolation and sequencing of TCRs

Total RNA was isolated from T cell clones using an RNeasy Mini Kit (QIAGEN), and cDNA was synthesized using SuperScript III Reverse Transcriptase (Invitrogen) according to the manufacturer's instructions. A multiplex PCR was used to amplify rearranged TCR transcripts, which were then cloned into pGEM-T Easy (Promega) and sequenced. TCR gene usage and CDR3 sequences were determined using IMGT/V-QUEST (16).

TCR clonotyping

Clonotypic analysis was performed as described previously, with minor modifications (17). Briefly, viable tetramer$^+$ CD4$^+$ T cells were sorted directly into 1.5-ml microtubes (Sarstedt) containing 100 μl RNAlater (Applied Biosystems), using a custom-modified FACSAria II flow cytometer (BD Biosciences). Unbiased amplification of all expressed *TRBV* gene products was conducted using a template-switch anchored RT-PCR with a 3′ C region primer (5′-TGGCTCAAACAAGGAGACCT-3′). Amplicons were subcloned, sampled, sequenced, and analyzed as described previously (18).

Mutagenesis, protein expression, and purification

HLA-DQ8-glia-α1 and TCRs were expressed via baculovirus-mediated insect cell and *Escherichia coli* expression, respectively (9, 19–21). The HLA-DQ8-glia-α1 construct contained a C-terminal enterokinase-cleavable (GenScript) leucine zipper domain incorporating a distal BirA recognition sequence for biotinylation and a polyhistidine tag for protein purification, which was removed prior to copurification with TCRs and subsequent crystallization (9). TCR point mutants were obtained via PCR mutagenesis, as described previously (9). Tetramers were assembled from biotinylated HLA-DQ8-glia-α1 and NeutrAvidin R-PE (Invitrogen), as described previously (9).

Crystallization, data collection, and processing

Crystallization was carried out using the hanging-drop vapor-diffusion method at 20°C. All TCR-HLA-DQ8-glia-α1 complexes were concentrated to 5–10 mg/ml in 10 mM Tris pH 8, 150 mM NaCl. Crystals of the TCR-HLA-DQ8-glia-α1 complexes were obtained by mixing 0.5 μl of each protein solution with 0.5 μl (1 μl for T316) of the following mother liquor solutions: 1) S13: 140 mM Na acetate, 0.1 M bis-tris propane pH 7.5, 15% polyethylene glycol (PEG) 8000; 2) L3: 80 mM Na acetate, 0.1 M bis-tris propane pH 6.5, 16% PEG8000; and 3) T316: 0.32 M $(NH_4)_2SO_4$, 0.1 M HEPES pH 7.8, 20% PEG3350. Prior to flash freezing in liquid nitrogen, crystals were cryoprotected by gradual transfer into mother liquor supplemented with 16–20% PEG400. Datasets were collected at 100 K on the MX2 beamline of the Australian Synchrotron (22), using an ADSC Quantum 315r detector. Data processing was carried out with Mosflm and Scala from the *CCP4* program suite (23).

Structure determination, refinement, and validation

The crystal structures were solved by molecular replacement in *PHASER* (24), using the coordinates of the SP3.4 TCR and HLA-DQ8-glia-α1 (9) as separate search models. Refinement, structure validation, and analysis were conducted as described previously (9, 10).

Accession numbers

The coordinates and structure factors for the SP3.4-HLA-DQ8-glia-α1, S13-HLA-DQ8-glia-α1, L3-HLA-DQ8-glia-α1, and T316-HLA-DQ8-glia-α1 complexes have been deposited in the Protein Data Bank (http://www.wwpdb.org/) with entry codes 4GG6, 4Z7U, 4Z7V, and 4Z7W, respectively.

Surface plasmon resonance

Equilibrium affinity constants of TCRs for HLA-DQ8-glia-α1 were determined via surface plasmon resonance, as described previously (9, 10).

Results

HLA-DQ8-glia-α1–specific T cell clones express a highly biased TCR repertoire

In a previous study, four of seven TCRs expressed by HLA-DQ8-glia-α1–specific CD4$^+$ T cell clones derived from six patients used TRBV9, whereas two of seven TCRs used TRBV6 (9). As these clones were isolated by limiting dilution from long-term biopsy cultures, however, this bias may not accurately represent the in vivo TCR repertoire. We therefore used HLA-DQ8-glia-α1 tetramers to identify and clone Ag-specific T cells expanded with minimal in vitro culture from the small intestines of *HLA-DQ8*$^+$ CD patients.

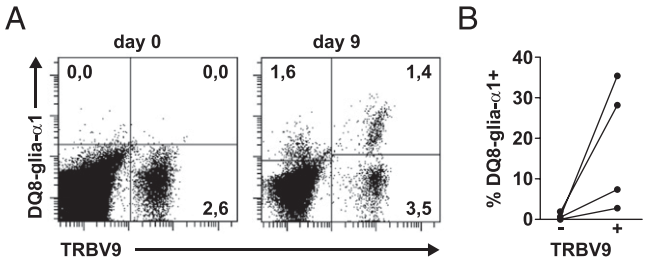

FIGURE 1. Detection of HLA-DQ8-glia-α-1 tetramer$^+$ T cells in short-term duodenal biopsy cultures from CD patients on a gluten-free diet. Biopsy samples from patients B, Bel, C, and Eve were cultured with TG2-treated gliadin for 4–11 d in the presence of IL-2 and IL-15 from day 5 onward. (**A**) Representative HLA-DQ8-glia-α-1 tetramer stains (patient Bel). CD4$^+$ cells within a live lymphocyte gate are shown, and numbers represent cell percentages within the quadrants. (**B**) Summary of staining data from the biopsy cultures, showing the frequencies of tetramer$^+$ cells within TRBV9$^-$ and TRBV9$^+$ CD4$^+$ T cells. Patient B (35% tetramer$^+$ of TRBV9$^+$ CD4$^+$), day 4 (no cytokines added); patient Bel (28%), day 9; patient C (7%), day 11; patient E (3%), day 9.

Multiple biopsy samples were obtained from four adult *HLA-DQ8*$^+$ CD patients on a gluten-free diet. Of these, 50% were digested with collagenase to release lymphocytes, which were then characterized directly ex vivo by flow cytometry. The other 50% were stimulated with a deamidated gliadin preparation and expanded for 4–11 d before flow cytometric analysis. No tetramer$^+$ cells were detected above background at day 0 (Fig. 1A). In contrast, tetramer$^+$ CD4$^+$ T cells were detected after short-term culture, predominantly within the TRBV9$^+$ compartment (Fig. 1B). These results demonstrate that the HLA-DQ8-glia-α1–specific TCR repertoire in primary biopsy material from CD patients is indeed strongly biased toward the use of TRBV9.

On the basis of tetramer staining and TRBV9 expression, single cells from all four subsets were sorted by flow cytometry and propagated. Only T cell clones generated from tetramer$^+$ cells were HLA-DQ8-glia-α1–specific. These clones stained uniformly with the HLA-DQ8-glia-α1 tetramer, and staining was abolished by the addition of an HLA-DQ–specific Ab (SPV-L3). No blocking effects were observed with a CD4-specific Ab (data not shown). Our tetramer-based approach therefore enabled the accurate selection of HLA-DQ8-glia-α1–specific T cells after short-term culture of biopsy material from *HLA-DQ8*$^+$ CD patients.

Next, we sequenced the TCRs expressed by these HLA-DQ8-glia-α1–specific T cell clones (Table I). A total of 11 new TCR sequences were identified in addition to the 7 reported previously (9). Of these 18 sequences, 9 expressed TRBV9, 10 expressed TRAV26-1/2, and 8 coexpressed TRBV9 and TRAV26-1/2. Furthermore, seven clones expressed TRBV6-1. Of these, two coexpressed TRAV26-1 and three coexpressed TRAV8-3. Thus, although most TRAV26$^+$ clones were TRBV9$^+$ and vice versa, TRAV26 and TRBV9 were also found paired with other TRBV or TRAV segments. These results extend our previous observations on the frequent use of TRBV9 and TRAV26 by HLA-DQ8-glia-α1–specific T cells (9), and further indicate that TRBV6-1 is also preferentially used by T cells with this specificity.

We previously noted the presence of a non–germline-encoded arginine (Arg) in the CDR3α region of four TRBV9$^+$ T cell clones (9). Closer inspection of the current sequences revealed that the majority of TCRs (17 of 18) contained an Arg in either the CDR3α or the CDR3β loops, which in most cases (14 of 17) was not germline-encoded (Table I). The presence of a CDR3α Arg was strongly associated with TRBV9 (nine of nine TCRs), in contrast to other TRBV segments (two of nine TCRs). Strikingly, the majority of TRBV9$^-$ chains contained a CDR3β Arg (six of nine TCRs). These findings suggest that a CDR3-encoded Arg contributes to TCR recognition of HLA-DQ8-glia-α1. It is also notable that some CDR3 sequences were highly similar between TCRs. For example, L3-12 and E995 shared an identical CDR3α, C2501 and Bel501 shared an identical CDR3β, and T316 and B403 expressed near-identical CDR3α and CDR3β loops.

To further characterize the TRBV repertoire expressed by HLA-DQ8-glia-α1–specific T cells, we sorted tetramer$^+$/TRBV9$^+$, tetramer$^+$/TRBV9$^-$, tetramer$^-$/TRBV9$^-$, and tetramer$^-$/TRBV9$^+$ cells from three biopsy lines for clonotypic analysis. In total, 811 TRB sequences were obtained, 508 of which were derived from tetramer$^+$ cells. Of these 508 sequences, 247 were TRBV9$^+$, 184 were TRBV6-1$^+$, 74 were TRBV20-1$^+$, and 3 were TRBV11-2$^+$. The tetramer$^+$/TRBV9$^+$ cell populations yielded only TRBV9$^+$ sequences with highly skewed, oligoclonal hierarchies (Table II). Similarly, the tetramer$^+$/TRBV9$^-$ cell populations yielded a limited number of sequences dominated by either TRBV6-1 or TRBV20-1. In two patients, the majority of CDR3β sequences obtained from these tetramer$^+$/TRBV9$^-$ cells contained a non–germline-encoded Arg. In contrast, the tetramer$^-$ cells yielded

Table I. *TRAV* and *TRBV* gene usage and CDR3 sequences of HLA-DQ8-glia-α1–restricted TCRs

Clone (#)	TRAV	TRBV	CDR3α	CDR3β	TRAJ	TRBD	TRBJ
SP3.4 (1)[a]	26-2*01	9*01	CILRDGRGGADGLTF	CASSVAVSAGTYEQYF	45*01	1*01	2-7*01
L3-12 (1)[a]	26-2*01	9*01	CILRDSRAQKLVF	CASSAGTSGEYEQYF	54*01	1*01	2-7*01
E995 (6)	26-2*01	9*01	CILRDSRAQKLVF	CASSVGVAGEYEQYF	54*01	2*02	2-7*01
S13 (1)[a]	26-2*01	9*01	CILRDRSNQFYF	CASSTTPGTGTETQYF	49*01	1*01	2-5*01
B501 (6)	26-2*01	9*01	CILRDDRGGKLIF	CASSAGPQAGTQYF	23*01	1*01	2-5*01
B503 (2)	26-2*01	9*01	CILRGRDNYGQNFVF	CASSVESGISNNEQFF	26*01	2*02	2-1*01
C2501 (2)	26-1*01	9*01	CIVTGRGSTLGRLYF	CASSVEVSGNTIYF	18*01	1*01	1-3*01
Bel501 (1)	26-1*01	9*01	CIVHGRQTGANNLFF	CASSVEVSGNTIYF	36*01	2*02	1-3*01
B401 (1)	26-1*01	6-1*01	CIVRGRNAGNMLTF	CASSETLGNEQYF	39*01	1*01	2-7*01
C1401 (3)	26-1*01	6-1*01	CIVRVANLVGNTGKLIF	CASSEGPDLAKNIQY	37*01	1*01	2-4*01
T316 (1)[a]	8-3*01	6-1*01	CAVGETGANNLFF	CASSEARRYNEQFF	36*01	2*02	2-1*01
B403 (2)	8-3*01	6-1*01	CAVGDTGANNLFF	CASSELRRYNEQFF	36*01	2*02	2-1*01
B452 (1)	8-3*01	6-1*01	CAVVNTGTASKLTF	CASSEGPTGRAGNTIYF	44*01	1*01	1-3*01
LS1.2 (1)[a]	17*01	6-1*01	CATDFPGTASKLTF	CASSEALPGRSGNTIYF	44*01	1*01	1-3*01
Bel403 (1)	4*01	6-1*01	CLVGDGISGGYNKLIF	CASSEGLAVAKNIQYF	4*01	2*01	2-4*01
Bel401 (2)	20*01	20-1*01	CAVMVQGAQKLVF	CSASRAGDFSTDTQYF	54*01	2*02	2-3*01
SP4.6 (1)[a]	38-2	9*01	CAYRSARGARLMF	CASSVAVSAGTYEQYF	31*01	1*01	2-7*01
S16 (1)[a]	13-1*02	4-2*01	CAGGSSNTGKLIF	CASSQDIRNTGELFF	37*01	2*01	2-2*01

Numbers in parentheses indicate the number of clones with this TCR sequence obtained from the patient. Non–germline-encoded residues in CDR3α/β are underlined.

[a]Previously reported in Ref. 9.

Table II. Clonotypic analysis of HLA-DQ8-glia-α1–specific CD4$^+$ T cells isolated from small-intestinal biopsy specimens

tet+ TRBV9+

	TRBV	CDR3	TRBJ	Freq (%)
B 88	9	CASSAGPQAGTQY	2-5	95.45
	9	CASSVEGGGTDTQY	2-3	2.27
	9	CASSVESGISNNEQF	2-1	1.14
	9	CASSAGPLAGTQY	2-5	1.14

	TRBV	CDR3	TRBJ	Freq (%)
C 83	9	CASSVEVSGNTIY	1-3	68.67
	9	CASSVEVMGSAQY	2-3	30.12
	9	CVSSVEVSGNTIY	1-3	1.20

	TRBV	CDR3	TRBJ	Freq (%)
Be 76	9	CASSVEGGGTGELF	2-2	34.21
	9	CASSVAPGSDTQY	2-3	32.89
	9	CASSVEVSGNTIY	1-3	15.79
	9	CASSVEVIGNTIY	1-3	10.53
	9	CASSVEVGFDTQY	2-3	5.26
	9	CAGSVAPGSDTQY	2-3	1.32

tet+ TRBV9-

	TRBV	CDR3	TRBJ	Freq (%)
B 89	6-1	CASSESGRGGNEQF	2-1	44.94
	6-1	CASSEAPSAKNIQY	2-4	23.60
	6-1	CASSELRRYNEQF	2-1	23.60
	4-2	CASSPGTRHTDTQY	2-3	7.87

	TRBV	CDR3	TRBJ	Freq (%)
	6-1	CASSEGPDLAKNIQY	2-4	79.78
C 89	6-1	CASSEARPYNEQF	2-1	16.85
	6-1	CVSSEGPDLAKNIQY	2-4	1.12
	6-1	CASSEGPDPAKNIQY	2-4	1.12
	6-1	CAGSEGPDLAKNIQY	2-4	1.12

	TRBV	CDR3	TRBJ	Freq (%)
	20-1	CSASRAGDFSTDTQY	2-3	85.54
	6-1	CASSEGPDLAKNIQY	2-4	7.23
Be 83	11-2	CASSLVRETEAF	1-1	3.61
	20-1	CSASRAGDFSADTQY	2-3	1.20
	20-1	CSASRAGDFSTDAQY	2-3	1.20
	20-1	CSTSRAGDFSTDTQY	2-3	1.20

ID	Sequence alignment
	C A S S V E V S G N T I Y
Be	tgtgccagcagcgtcgaggtctctggaaacaccatatat
C	----------a----------

ID	Sequence alignment
	C A S S E G P D L A K N I Q Y
Be	tgtgccagcagtgaagggccagatctagccaaaaacattcagtac
C	----------t-----c----------
C	----------g--t--c--c--g----------
C	----------t-----c--g----------

TRBV and *TRBJ* gene usage, CDR3 amino acid sequence, and relative frequency of HLA-DQ8-glia-α1–specific CD4$^+$ T cell clonotypes sorted as distinct tetramer (tet)$^+$/TRBV9$^+$ and tetramer$^+$/TRBV9$^-$ populations from small-intestinal biopsy lines (*upper panels*). Colors denote identical sequences differentially encoded at the nucleotide level (*bottom panels*).

a far more diverse set of TRB sequences in which no single clonotype was overrepresented. Consistent with the T cell clone data, highly prevalent public TRBV9 and TRBV6-1 clonotypes were detected in the tetramer$^+$ repertoires. Of note, these clonotypes were differentially encoded at the nucleotide level both within and between patients, indicating selection at the protein level (Table II). Moreover, with one exception, the TRB sequences present in the panel of T cell clones were also found in the bulk populations (Table II). Together, these data provide clear evidence for the selection of a biased HLA-DQ8-glia-α1–specific TCR repertoire in patients with CD.

TRBV9$^+$ and TRBV9$^-$ T cell clones display similar reactivity against HLA-DQ8-glia-α1

Deamidation of particular glutamine residues in gluten-derived peptides is generally required for optimal T cell reactivity. In the case of the DQ8-glia-α1 peptide, specific deamidation of glutamine at position (p) 1 and/or p9 leads to enhanced antigenicity (7). To determine the deamidation dependence of our T cell clones, we measured the proliferation of seven TRAV26/TRBV9$^+$ and seven TRAV26/TRBV9$^-$ clones in response to the native DQ8-glia-α1 peptide and variants thereof in which the glutamine at p1 and/or p9 was replaced with glutamic acid (Fig. 2A, 2B). In agreement with previous results, most clones responded poorly to the native peptide and better to the modified peptides; responses to the single-substituted peptides were generally lower than those to the double-substituted peptide. Overall, no significant differences were found in the response profiles between TRBV9$^+$ and TRBV9$^-$ clones (Fig. 2C). Thus, deamidation of the DQ8-glia-α1 peptide enhances T cell recognition in a clonotype-independent manner.

Next, we tested the fine specificity of our T cell clones against alanine-substituted variants of the DQ8-glia-α1 peptide (sequence SG**EGSFQPSQE**NP; p1–p9 core in bold) (Fig. 3). For the TRBV9$^+$ T cell clones, replacement of p1-Glu by Ala was generally tolerated, but an analogous substitution at p9-Glu led to the loss of T cell recognition in all cases (Fig. 3A). Further, replacement of the residues at p3, p8, and, to a lesser extent, p5 greatly decreased T cell recognition. The impact of substitutions at p2 and p6 was highly variable, whereas replacement of the p4 and p7 residues was generally tolerated. Strikingly, replacement of p10-Asn and p11-Pro abrogated T cell recognition, whereas the amino acids at p1 and p2 could be freely replaced. These data indicate that the TRBV9$^+$ TCRs interact with the C-terminal part of the peptide (Fig. 3A).

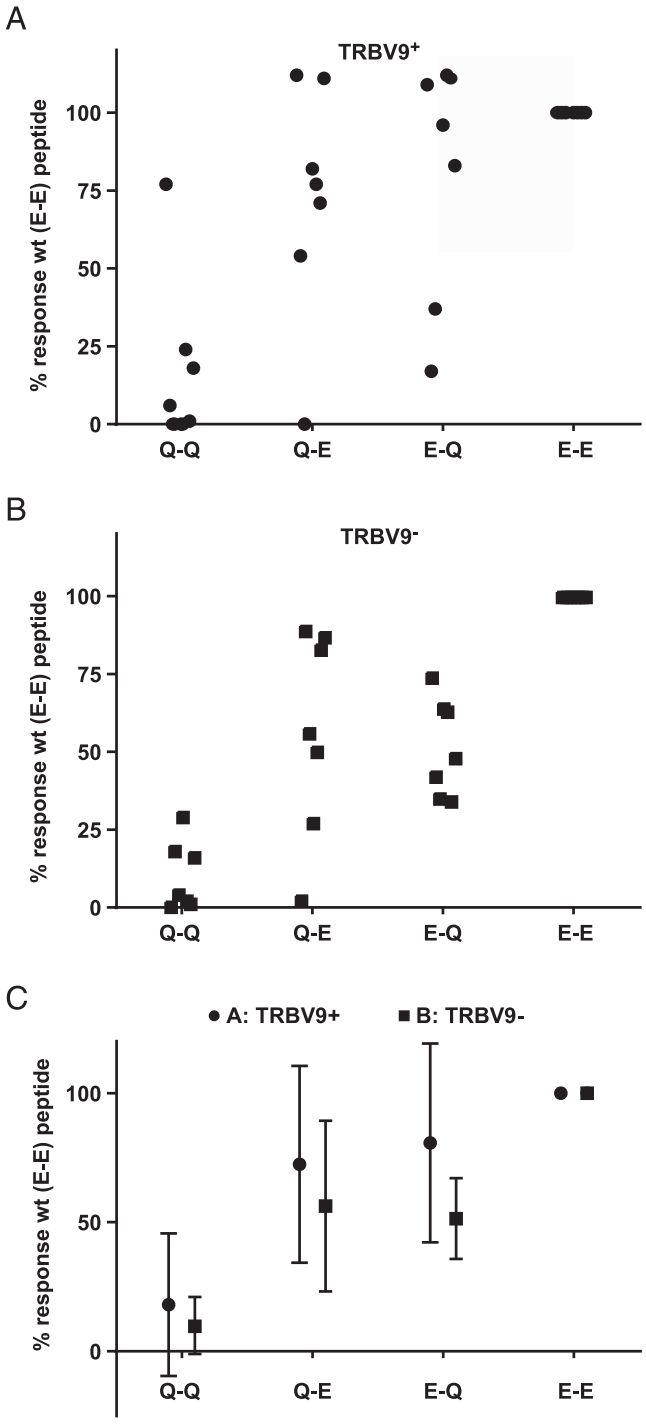

FIGURE 2. Deamidation dependence of TRBV9$^+$ and TRBV9$^-$ T cell clones. T cell clones were incubated with HLA-DQ8 homozygous EBV-LCLs in the presence of 6 μg/ml of the indicated peptides. Q-Q: SGQGSFQPSQQNP; Q-E: SGQGSFQPSQENP; E-Q: SGEGSFQPSQQNP; E-E [wild-type (wt)]: SGEGSFQPSQENP. ^{3}H-thymidine incorporation was measured during the final 17 h of a 72-h incubation and normalized to the response against the double-deamidated peptide, set at 100% [absolute average counts in brackets]. (**A**) TRBV9$^+$ clones (n = 7: B502 [43,336], B503 [2688], C2501 [33,710], S13 [14,833], Bel501 [22,891], E995 [29,688], L3-12 [20,090]). (**B**) TRBV9$^-$ clones (n = 7: C1401 [571], S16 [10,341], T316 [8416], B403 [382], B401 [39,250], B452 [537], Bel402 [38,651]). (**C**) Summary of all clones, showing means ± SD. For reference, the deamidation dependence of clones S13, L3-12, S16, and T316 was tested previously using a shorter version of the DQ8-glia-α1 epitope (SGEGSFQPSQEN), with similar results (9).

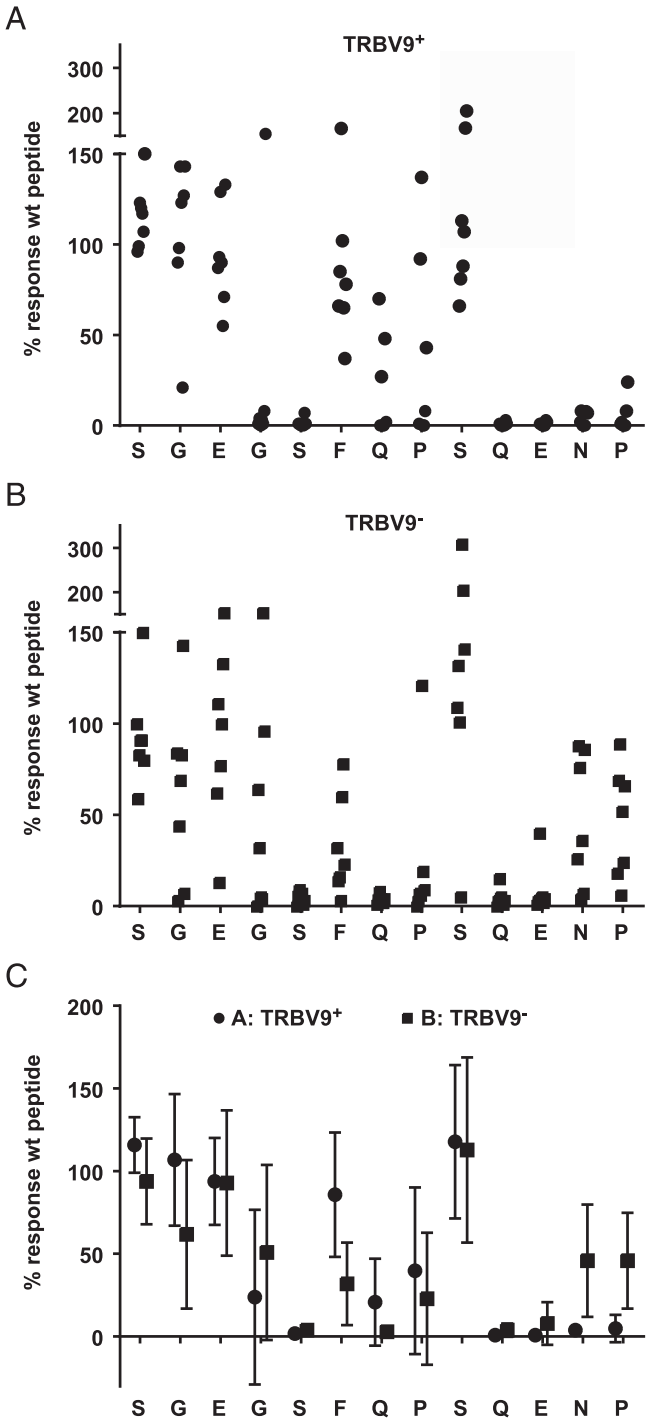

FIGURE 3. Responses of TRBV9$^+$ and TRBV9$^-$ T cell clones against alanine-substituted variants of the DQ8-glia-α1 peptide. T cell clones were incubated with HLA-DQ8 homozygous EBV-LCLs in the presence of 6 μg/ml of the indicated peptides, in which amino acid residues in the DQ8-glia-α1 epitope (SGEGSFQPSQENP) were substituted with alanine at the indicated positions. ^{3}H-thymidine incorporation was measured during the final 17 h of a 72-h incubation and normalized to the response against the nonsubstituted peptide, set at 100% [absolute average counts in brackets]. (**A**) TRBV9$^+$ clones (n = 7: B502 [44,592], B503 [4890], C2501 [19,960], S13 [13,471], Bel501 [26,734], E995 [26,651], L3-12 [4637]). (**B**) TRBV9$^-$ clones (n = 7: C2405 [2320], S16 [4637], T316 [981], B403 [923], B401 [43,871], B452 [3086], Bel401 [6130]). (**C**) Summary of all clones, showing means ± SD. For reference, responses to alanine-substituted peptides for clones T316, S13, and L3-12 were tested previously using a shorter version of the DQ8-glia-α1 epitope (SGEGSFQPSQEN), with similar results (15).

Similar to the TRBV9$^+$ T cell clones, the TRBV9$^-$ T cell clones tolerated replacement of p1-Glu but not p9-Glu, and Ala substitutions at p3, p5, and p8 had the greatest impact on T cell reactivity (Fig. 3B). In contrast to the TRBV9$^+$ T cell clones, however, the TRBV9$^-$ clones were less sensitive to replacement of the residues at p10 and p11, indicating that these amino acids were less important for the interaction with TRBV9$^-$ TCRs. Nevertheless, comparable reactivity patterns were observed for the TRBV9$^+$ and TRBV9$^-$ T cell clones (Figs. 2C, 3C), suggesting common TCR contact residues in HLA-DQ8-glia-α1.

HLA-DQ8-glia-α1–specific TCRs bind Ag with high affinities

Using surface plasmon resonance, we measured the binding affinity of the public TRAV8-3/TRBV6-1 TCR T316 for HLA-DQ8-glia-α1. Like previously reported TRBV9$^+$ TCRs (1.1–11.4 μM; Ref. 9), this TRBV9$^-$ TCR bound HLA-DQ8-glia-α1 with relatively high affinity (2.1 ± 0.1 μM) (Supplemental Figure 1). Affinities of this magnitude are typically associated with TCRs that recognize nonself/microbial epitopes (25, 26).

We previously observed how HLA-DQ8-glia-α1 recognition by a TRAV26-2/TRBV9 TCR and HLA-DQ2-glia-α2 recognition by three TRAV26-1/TRBV7-2 TCRs depended on a CDR3-encoded Arg (9, 10). In this study, we noted similarly positioned non–germline-encoded Arg residues in the CRD3β loops of several HLA-DQ8-glia-α1–specific TRAV26$^-$/TRBV9$^-$ TCRs (Table I). To test the hypothesis that selection of a central Arg is a hallmark of CD-associated TCRs, we mutated the CDR3β Arg present in the unrelated TCR T316 (CDR3β Arg^{110}). The mutation CDR3β Arg→Ala led to a complete loss of binding, whereas the conservative Arg→Lys mutation caused a >20-fold decrease in affinity for HLA-DQ8-glia-α1 (Supplemental Fig. 1). Similarly, the mutation CDR3α Arg→Ala abrogated binding (K_d >200 μM) of the L3-12 (data not shown), S13 (data not shown), and SP3.4 (9) TRAV26-2/TRBV9 TCRs. Thus, the CDR3-encoded Arg plays a major role in the HLA-DQ8-glia-α1–specific T cell response.

Conserved docking mode of TRAV26-2/TRBV9 TCRs onto HLA-DQ8-glia-α1

Next, we determined the structures of two TRAV26-2/TRBV9 TCRs (L3-12 and S13) in complex with HLA-DQ8-glia-α1 (Table III, Supplemental Tables I, II). Despite clear differences in both length and amino acid composition of the CDR3α and CDR3β loops present in the L3-12, S13, and previously described SP3.4 (9) TCRs (Table I), the structures of these TCRs in complex with HLA-DQ8-glia-α1 revealed highly similar footprints and docking angles onto HLA-DQ8-glia-α1 (Fig. 4A–C), as well as overall buried surface areas (BSA) of ~900 Å^2. Within this consensus footprint, the CDR1β-Leu^{37} and CDR2β-Tyr^{57} residues characteristic of the TRBV9 chain were positioned almost identically with respect to both the peptide and HLA-DQ8 (Fig. 5D).

The structures revealed a van der Waals' (vdw) interaction between CDR1β-Leu^{37} and p11-Pro of the peptide (Fig. 5A), Ala substitution of which abrogated TCR recognition (Fig. 3). Nevertheless, the CDR3α and CDR3β loops played a dominant role in the interactions with peptide (Fig. 5A, 5C, 5E). The most extensive peptide interactions occurred with p8-Gln, which interacted with multiple residues in CDR1β, CDR2β, and CDR3β, and which was also crucial for T cell recognition (Fig. 3). Of note, the orientation of the non–germline-encoded CDR3α Arg, stabilized by a salt bridge to the adjacent Asp^{108}, was conserved in all three complexes (Fig. 5A, 5C, 5E, 5F), and its interaction with peptide centered on p3-Ser, essential for the induction of T cell proliferation (Fig. 3). The interface of CDR3α and HLA-DQ8 was largely mediated by HLA-DQ8 Phe$^{58\alpha}$ (Fig. 5F). Together, these findings indicate highly conserved interactions between TRBV9$^+$ TCRs and HLA-DQ8-glia-α1.

Table III. Data collection and refinement statistics

	L3	S13	T316
Wavelength (Å)	0.95369	0.95370	0.95370
Resolution range (Å)	38.80–2.65 (2.745–2.65)	39.53–2.70 (2.78–2.70)	85.69–2.89 (3.00–2.90)
Space group	P 1	P 21 21 21	P 1 21 1
Unit cell			
a b c (Å)	56.51 76.961 132.279	83.454 123.813 223.086	66.623 200.518 87.183
α β γ (°)	93.87 89.47 105.09	90 90 90	90 100.63 90
Unique reflections	61285 (6102)	60719 (5529)	45344 (3955)
Multiplicity	2.6 (2.62)	4.1 (3.6)	4.1 (4.0)
Completeness (%)	98.28 (97.96)	94.41 (87.19)	90.59 (79.16)
Mean I/σ(I)	12.38 (2.21)	7.5 (2.3)	11.13 (3.34)
Wilson B-factor	45.66	51.98	42.54
R-merge	0.06 (0.35)	0.107 (0.502)	0.117 (0.421)
R-work	0.1910 (0.2651)	0.1848 (0.2593)	0.2477 (0.3312)
R-free	0.2317 (0.3286)	0.2279 (0.3307)	0.2681 (0.3743)
Number of atoms	13076	13076	12981
Macromolecules	12595	12689	12704
Ligands	146	124	173
Water	335	263	104
Protein residues	1615	1620	1622
RMS (bonds)	0.011	0.013	0.010
RMS (angles)	1.60	1.81	1.47
Ramachandran			
Favored (%)	97	96	95
Outliers (%)	0.13	0.13	0.13
Clashscore	2.12	3.27	1.98
Average B-factor	62.80	67.60	59.40
Macromolecules	62.60	67.50	59.50
Ligands	125.10	112.70	68.50
Solvent	42.80	49.00	26.90

Statistics for the highest-resolution shell are shown in parentheses.
RMS, root mean square deviation from ideal.

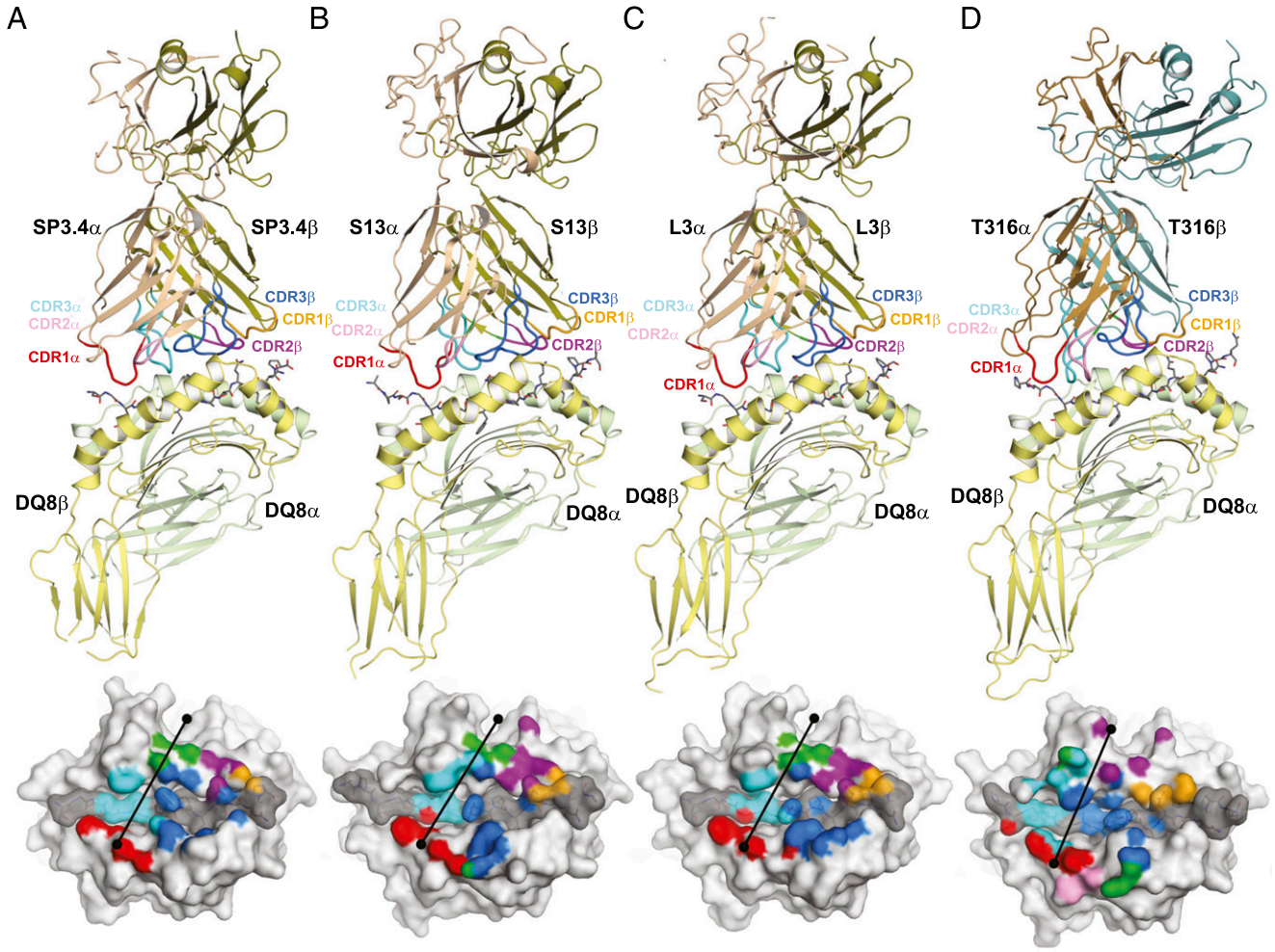

FIGURE 4. Structural overview and TCR footprints of TCR-HLA-DQ8-glia-α1 complexes. (**A**) SP3.4 (previously reported in Ref. 9, PDBj entry code 4GG6), (**B**) S13, (**C**) L3-12, and (**D**) T316. Each complex structure is shown in cartoon representation with the peptide as a stick model and the TCR on top. CDR loops 1α, 2α, 3α, 1β, 2β, and 3β are highlighted in red, pink, cyan, orange, magenta, and blue, respectively. The corresponding TCR footprints on HLA-DQ8-glia-α1 are shown in surface representation (bottom) with the TCR docking angle shown as a black line connecting the α and β variable domain center of mass positions (black spheres). HLA-DQ8 is colored light gray with the DQ8-glia-α1 peptide in dark gray. TCR contact atoms are colored according to the color of the nearest CDR loop; TCR framework contacts are colored green.

Structure of a TRAV8-3/TRBV6-1 TCR-HLA-DQ8-glia-α1 complex

The TRBV6-1$^+$ TCRs were overrepresented in HLA-DQ8-glia-α1–specific T cell populations and incorporated TRAV8-3 in three of seven T cell clones (Table I). To elucidate the molecular basis for TRBV6-1 usage, we determined the structure of the TRAV8-3/TRBV6-1 T316 TCR-HLA-DQ8-glia-α1 complex (Table III, Supplemental Table III). The overall docking orientation of this TRBV6-1$^+$ TCR was similar to that of the TRBV9$^+$ TCRs (SP3.4, L3-12, and S13), but the center of mass was shifted toward the N terminus of the peptide, and the interface BSA of 1150 Å^2 was ∼25% larger compared with the TRBV9$^+$ TCRs (Fig. 4D). However, the relative BSA contributions of the T316 TCR α-chain and β-chain (45% and 55%, respectively) and the CDR3 loops (∼21% for CDR3α and 29% for CDR3β) were broadly similar to those of the TRBV9$^+$ TCRs (∼23% for CDR3α and 30% for CDR3β).

The HLA-DQ8 residues interacting with the germline-encoded regions of T316 included, for the most part, the consensus footprint of the germline-encoded portions of the TRAV26-2/TRBV9 TCRs. Despite this overlap, direct structural similarities in the germline-encoded regions of T316 and the TRBV9$^+$ TCRs were limited to the comparable backbone conformations of the CDR1 and CDR2 loops. To illustrate, the Thr$^{36\alpha}$ and Tyr$^{38\alpha}$ residues conserved between TRAV26-2 (Fig. 5B) and TRAV8-3 (Fig. 6A) had distinct interactions with the HLA-DQ8 β-chain.

In the T316 TCR-HLA-DQ8-glia-α1 complex, we observed TRBV6-1–encoded interactions involving Asn$^{28\beta}$ and Asn$^{37\beta}$ of the CDR1β loop (Fig. 6B). These interactions were spatially equivalent to Leu$^{37\beta}$ and Tyr$^{57\beta}$ in the TRBV9$^+$ TCRs (Fig. 5D). In the TRBV6-1 complex, Asn$^{37\beta}$ assumed the role of Tyr$^{57\beta}$ in the TRBV9 structures by H-bonding to p8-Gln while forming vdw contacts with the HLA-DQ8 α-chain via Thr$^{61\alpha}$, Ala$^{64\alpha}$, and Val$^{65\alpha}$ (Fig. 6B, 6E). Asn$^{28\beta}$ followed the interaction pattern observed for the TRBV9-encoded Leu$^{37\beta}$ by H-bonding to both p8-Gln (Fig. 6E) and His$^{68\alpha}$ of the HLA-DQ8 α-chain (Fig. 6B). Thus, despite the low homology between TRBV6-1 and TRBV9, the T316 TCR ternary complex encompassed several germline-encoded features that closely mimicked the interactions of critical germline-encoded residues in the TRBV9$^+$ TCRs.

Compared with the TRBV9$^+$ TCRs, the positions of the T316 TCR CDR3 loops were shifted toward the N terminus of the peptide. The CDR3α loop formed an extensive interface with

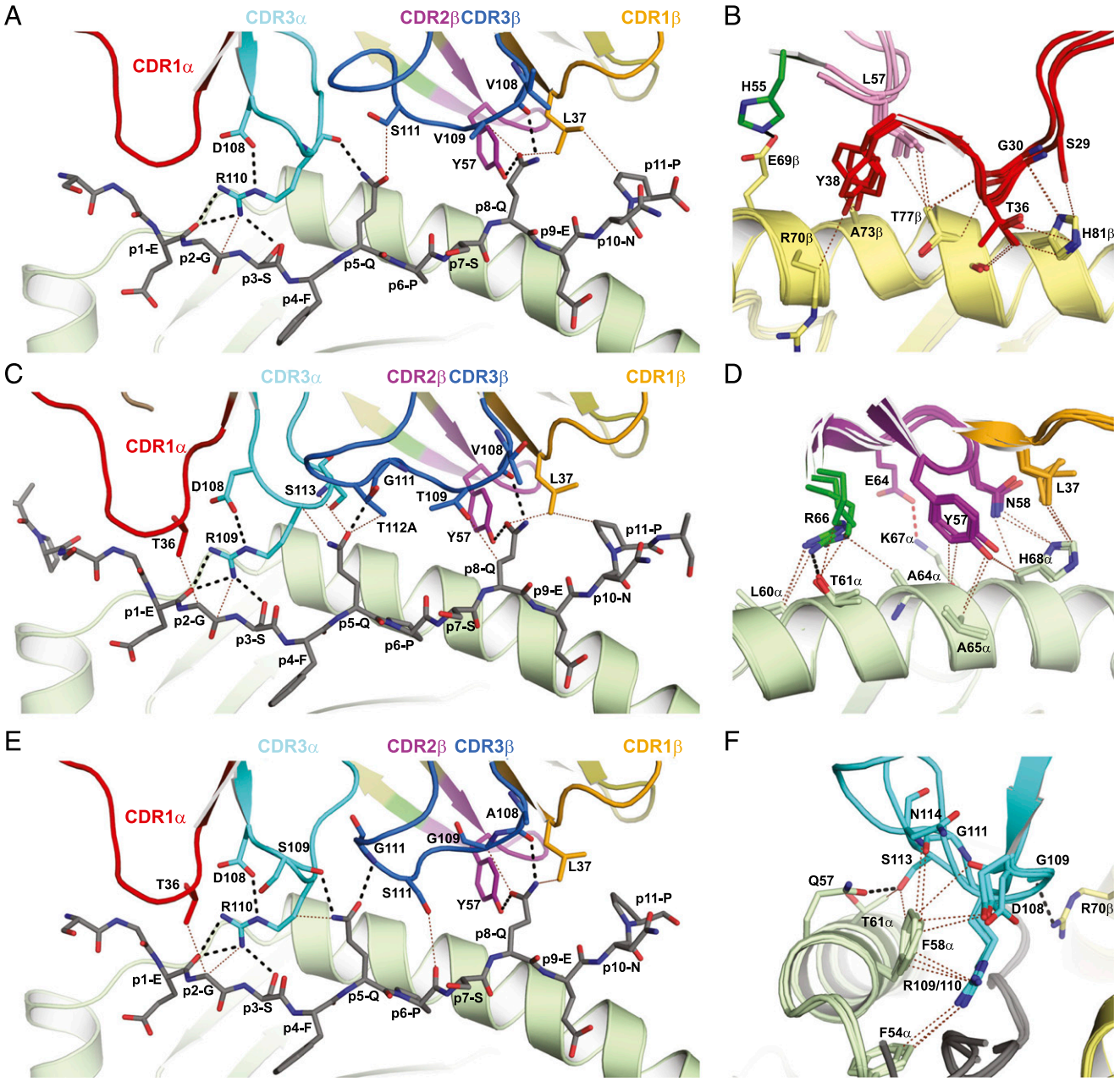

FIGURE 5. Interface comparison of TRBV9$^+$ TCRs recognizing HLA-DQ8-glia-α1. CDR loops 1α, 2α, 3α, 1β, 2β, 3β and framework residues are highlighted in red, pink, cyan, orange, magenta, blue and green, respectively. TCR–peptide contacts are shown separately for (**A**) SP3.4, (**C**) S13, and (**E**) L3-12. (A, C, and E) The non–germline-encoded CDR3α Arg residue is stabilized by a salt bridge to the adjacent Asp^{108} and contacts the peptide in the same positions in all three TRBV9$^+$ TCR-HLA-DQ8-glia-α1 complexes. Differences in the CDR3α and CDR3β loops of the three complexes are mainly manifested in the interface contacts involving p5-Gln. (**B**, **D**, and **F**) Contacts between the CDR loops and HLA-DQ8 are shown as a structural overlay of the three TRBV9$^+$ complexes. The overlays show a high degree of conservation in side chain positions and interactions between the CDR1 and CDR2 germline-encoded regions and HLA-DQ8. (B) HLA-DQ8 contacts of CDR1α and CDR2α. (D) HLA-DQ8 contacts of CDR1β and CDR2β. (F) The interface of CDR3α and HLA-DQ8 is largely mediated by HLA-DQ8 Phe$^{58\alpha}$. Despite sequence differences in the non–germline-encoded CDR3α between the three TRBV9$^+$ complexes, the position and interactions of Arg^{110} are highly conserved.

HLA-DQ8, whereas interactions with the peptide were limited to contacts with p1-Gly and p1-Glu. The CDR3β contacted HLA-DQ8 and lay on top of p5-Gln, contacting it via an H-bond with Asn$^{114\beta}$ and vdw interactions with Ala$^{109\beta}$ and Arg$^{110\beta}$, whereas p8-Gln contacted Glu$^{108\beta}$. Surprisingly, the CDR3β Arg^{110} was positioned similarly to the CDR3α Arg^{110} in the TRAV26-2/TRBV9 TCRs (Figs. 4, 5). Specifically, Arg$^{110\beta}$ reached deep into the peptide binding cleft and H-bonded to the side chain of p3-Ser and the peptide backbone, while interacting with the HLA-DQ8 α-chain via an H-bond to Asn$^{62\alpha}$ and a vdw contact with Phe$^{58\alpha}$ (Fig. 6D). Moreover, the position of Arg$^{110\beta}$ was stabilized through a hydrogen bond with the adjacent CDR3β Tyr^{113} (Fig. 6D). Thus, the non–germline-encoded Arg$^{110\beta}$ in T316 engaged in an interaction pattern strikingly similar to that of the CDR3α Arg in the TRAV26-2/TRBV9 TCRs (Fig. 5A, 5C, 5E, 5F). Also similar to the TRBV9$^+$ TCRs, and in agreement with the functional data, substantial interactions were noted between the TRBV6-1$^+$ TCR and p3-Ser, p5-Gln, and p8-Gln in DQ8-glia-α1, explaining the conserved fine specificity of these distinct TCRs.

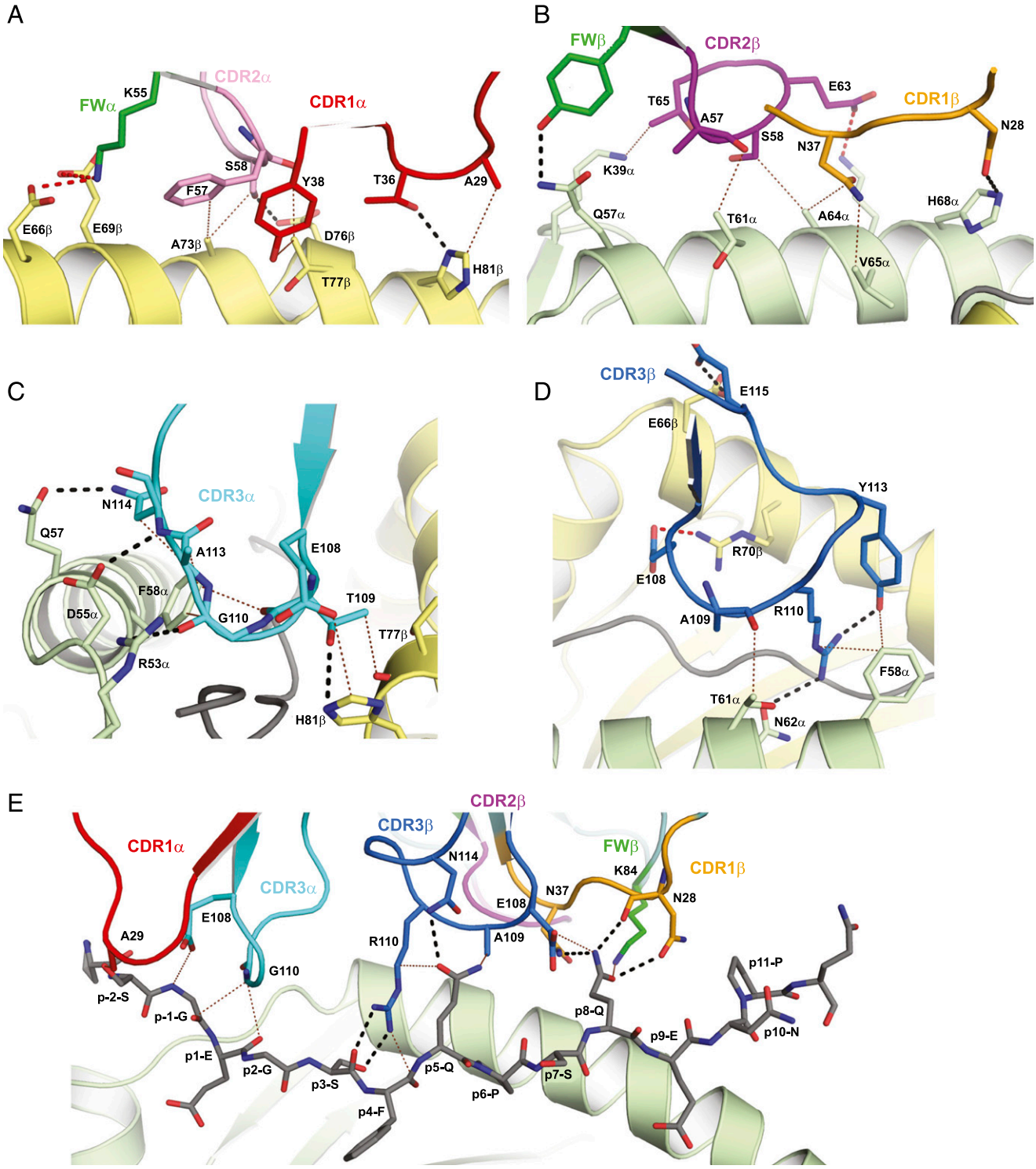

FIGURE 6. Interface of the TRBV6-1^{+} T316 TCR recognizing HLA-DQ8-glia-α1. CDR loops 1α, 2α, 3α, 1β, 2β, 3β and framework residues are highlighted in red, pink, cyan, orange, magenta, blue and green, respectively. (**A** and **B**) The interactions of the CDR1 and CDR2 germline-encoded regions of T316 with HLA-DQ8 include the consensus footprint of the TRBV9^{+} TCRs, with the exception of a peripheral contact involving HLA-DQ8 Leu$^{60\alpha}$ (refer to Fig. 5D). (A) CDR1α and CDR2α form additional interactions with HLA-DQ8 Glu$^{66\beta}$ and Asp$^{76\beta}$. (B) CDR1β and CDR2β form additional interactions with HLA-DQ8 Lys$^{39\alpha}$, Gln$^{57\alpha}$, and Lys$^{70\alpha}$. (**C**) The interface of CDR3α with the HLA-DQ8 α-chain involves extensive contacts with Phe$^{58\alpha}$, similar to the analogous interface in the TRBV9^{+} TCRs. (**D**) Interactions of CDR3β with HLA-DQ8. (**E**) Interactions between T316 and the DQ8-glia-α1 peptide.

Discussion

Gluten-specific T cell responses play a crucial role in the pathogenesis of CD (1, 2, 4), and recent studies indicate that immunodominant gluten-derived peptides are targeted in vivo by T cell populations with biased TCR repertoires (9–12). In this article, we provide an in-depth analysis of the HLA-DQ8-glia-α1–specific TCR repertoire in affected duodenal tissue. Two TRBV regions (TRBV9, TRBV6-1) and one TRAV region (TRAV26) were

highly prevalent, and the vast majority of TCRs contained a non–germline-encoded Arg in either their CDR3α (TRBV9$^+$ TCRs) or CDR3β (TRBV9$^-$ TCRs) loops.

The crystal structures of two TRBV9$^+$ TCRs and one TRBV9$^-$ TCR revealed similar footprints on the HLA-DQ8-glia-α1 complex, with amino acid residues characteristic of TRBV9 and TRBV6-1 making critical contributions to the interaction. Furthermore, the docking mode of the TRBV9$^-$ TCR was shifted compared with the TRBV9$^+$ TCRs, thereby conserving specific interactions between the CDR3-encoded Arg and the N terminus of the peptide. Together, these structures explain the similar peptide recognition patterns observed across HLA-DQ8-glia-α1–specific T cell clones with divergent TCR sequences.

The structures of the complexes between HLA-DQ8-glia-α1 and the TRAV26-2/TRBV9 TCRs SP3.4, L3-12, and S13 were highly similar, suggesting an archetypal interaction for all such TCRs carrying an Arg in the CDR3α loop. Moreover, an analogous interface with HLA-DQ8-glia-α1 was observed for the TRBV9$^-$ T316 TCR, which displayed an alternative docking mode likely representative of other TCRs with an Arg in the CDR3β loop. These interpretations are reinforced by the primary sequence analysis, which revealed that the L3-12 and E995 TCRs incorporate an identical CDR3α, whereas the C2501 and Bel501 TCRs incorporate an identical CDR3β. Despite the two docking modes, TRBV9$^+$ and TRBV9$^-$ T cell clones exhibited similar reactivity patterns against a panel of alanine-substituted DQ8-glia-α1 peptides. Substitutions at p3, p5, and p8 dramatically impaired T cell reactivity, consistent with the structural data showing that these residues act as major TCR contact sites. Thus, the available structures provide novel insights into the two major docking modes by which these TCRs interact with HLA-DQ8-glia-α1.

Similarities exist between the T cell responses to HLA-DQ8-glia-α1 and HLA-DQ2.5-glia-α2, particularly with regard to TRAV26 usage and the presence of a CDR3-encoded Arg. Although TRAV26-1 frequently pairs with TRBV7-2 in HLA-DQ2.5-glia-α2–specific T cells, HLA-DQ8-glia-α1–specific T cells use either TRAV26-1 or TRAV26-2, mostly in combination with TRBV9. The structures of the SP3.4 (9), S13, and L3-12 TCRs in complex with HLA-DQ8-glia-α1 revealed almost identical positioning of $Thr^{36\alpha}$ and $Tyr^{38\alpha}$ from CDR1α and $Leu^{57\alpha}$ from CDR2α above the HLA-DQ8 β-chain. Strikingly, the HLA-DQ2.5-glia-α2–specific TRAV26-1$^+$ TCRs are positioned in a very similar manner above the HLA-DQ2 β-chain (10). Of note, the HLA-DQ β-chain helix that interacts with TRAV26 is highly homologous between HLA-DQ2 (sequence E^{69}RKRAAVDRVCRH^{81}) and HLA-DQ8 (sequence E^{69}RTRAEVDTVCRH^{81}), allowing similar docking of the TRAV26$^+$ TCRs. Thus, our collective data provide a molecular basis for the frequent usage of TRAV26 by T cells specific for immunodominant gluten peptides in complex with HLA-DQ and highlight the critical importance of Arg within the CDR3 loop.

The presence of biased TCRs in every patient examined to date indicates an intimate association with disease pathogenesis. Although the potential TCR repertoire exceeds 10^{15} unique sequences (27, 28), the number of different TCRs present in a single individual may be as small as 25 million (29). It is therefore improbable that high-affinity public TCRs specific for immunodominant gluten peptides will be present in each and every individual at any given moment during life. Consequently, the emergence and/or expansion of such T cells is likely to be a crucial step toward disease development and may also be linked to differences in clinical presentation. It will therefore be important to compare and contrast naive and memory gluten-specific TCR repertoires, the latter at various stages of the disease, although this may be challenging given that gluten-specific CD4$^+$ T cells become less abundant in the duodenum with dietary treatment (30).

There are various indications that the biased TCRs described in this study have intermediate to high ligand affinities. First, direct measurements demonstrated TCR affinities for HLA-DQ8-glia-α1 in the range typically observed for nonself/microbial epitopes (1–10 μM). Second, tetramer staining and T cell activation were not inhibited by Abs to CD4. Third, low concentrations of the gliadin peptide were sufficient to elicit functional responses at the clonal level. Such T cells are therefore likely to contribute most significantly to the symptoms associated with gluten consumption. Analysis of the ternary complexes between public TCRs and HLA-DQ8-glia-α1 revealed shared structural features, an observation that extends in addition to HLA-DQ2-restricted TCRs isolated from CD patients (10). This knowledge could potentially be used to develop novel compounds that specifically target such public TCRs, in particular the interaction site that converges on the CDR3-encoded Arg. Effective elimination of T cells expressing high-affinity public TCRs, perhaps by coupling such compounds to toxins, might constitute a long-lasting treatment for CD.

Acknowledgments

We thank the staff of the Australian Synchrotron (beamlines MX1 and MX2) for assistance with data collection and Brenda Hartman for assistance with figure preparation.

Disclosures

The authors have no financial conflicts of interest.

References

1. Abadie, V., L. M. Sollid, L. B. Barreiro, and B. Jabri. 2011. Integration of genetic and immunological insights into a model of celiac disease pathogenesis. *Annu. Rev. Immunol.* 29: 493–525.
2. Di Sabatino, A., and G. R. Corazza. 2009. Coeliac disease. *Lancet* 373: 1480–1493.
3. Karell, K., A. S. Louka, S. J. Moodie, H. Ascher, F. Clot, L. Greco, P. J. Ciclitira, L. M. Sollid, and J. Partanen, European Genetics Cluster on Celiac Disease. 2003. HLA types in celiac disease patients not carrying the DQA1*05-DQB1*02 (DQ2) heterodimer: results from the European Genetics Cluster on Celiac Disease. *Hum. Immunol.* 64: 469–477.
4. Jabri, B., and L. M. Sollid. 2009. Tissue-mediated control of immunopathology in coeliac disease. *Nat. Rev. Immunol.* 9: 858–870.
5. Kim, C. Y., H. Quarsten, E. Bergseng, C. Khosla, and L. M. Sollid. 2004. Structural basis for HLA-DQ2-mediated presentation of gluten epitopes in celiac disease. *Proc. Natl. Acad. Sci. USA* 101: 4175–4179.
6. Molberg, O., S. N. Mcadam, R. Körner, H. Quarsten, C. Kristiansen, L. Madsen, L. Fugger, H. Scott, O. Norén, P. Roepstorff, et al. 1998. Tissue transglutaminase selectively modifies gliadin peptides that are recognized by gut-derived T cells in celiac disease. *Nat. Med.* 4: 713–717.
7. van de Wal, Y., Y. Kooy, P. van Veelen, S. Peña, L. Mearin, G. Papadopoulos, and F. Koning. 1998. Selective deamidation by tissue transglutaminase strongly enhances gliadin-specific T cell reactivity. *J. Immunol.* 161: 1585–1588.
8. Henderson, K. N., J. A. Tye-Din, H. H. Reid, Z. Chen, N. A. Borg, T. Beissbarth, A. Tatham, S. I. Mannering, A. W. Purcell, N. L. Dudek, et al. 2007. A structural and immunological basis for the role of human leukocyte antigen DQ8 in celiac disease. *Immunity* 27: 23–34.
9. Broughton, S. E., J. Petersen, A. Theodossis, S. W. Scally, K. L. Loh, A. Thompson, J. van Bergen, Y. Kooy-Winkelaar, K. N. Henderson, T. Beddoe, et al. 2012. Biased T cell receptor usage directed against human leukocyte antigen DQ8-restricted gliadin peptides is associated with celiac disease. *Immunity* 37: 611–621.
10. Petersen, J., V. Montserrat, J. R. Mujico, K. L. Loh, D. X. Beringer, M. van Lummel, A. Thompson, M. L. Mearin, J. Schweizer, Y. Kooy-Winkelaar, et al. 2014. T-cell receptor recognition of HLA-DQ2-gliadin complexes associated with celiac disease. *Nat. Struct. Mol. Biol.* 21: 480–488.
11. Qiao, S. W., M. Ráki, K. S. Gunnarsen, G. A. Løset, K. E. Lundin, I. Sandlie, and L. M. Sollid. 2011. Posttranslational modification of gluten shapes TCR usage in celiac disease. *J. Immunol.* 187: 3064–3071.
12. Qiao, S. W., A. Christophersen, K. E. Lundin, and L. M. Sollid. 2014. Biased usage and preferred pairing of α- and β-chains of TCRs specific for an immunodominant gluten epitope in coeliac disease. *Int. Immunol.* 26: 13–19.
13. Turner, S. J., P. C. Doherty, J. McCluskey, and J. Rossjohn. 2006. Structural determinants of T-cell receptor bias in immunity. *Nat. Rev. Immunol.* 6: 883–894.

14. Venturi, V., D. A. Price, D. C. Douek, and M. P. Davenport. 2008. The molecular basis for public T-cell responses? *Nat. Rev. Immunol.* 8: 231–238.
15. Kooy-Winkelaar, Y., M. van Lummel, A. K. Moustakas, J. Schweizer, M. L. Mearin, C. J. Mulder, B. O. Roep, J. W. Drijfhout, G. K. Papadopoulos, J. van Bergen, and F. Koning. 2011. Gluten-specific T cells cross-react between HLA-DQ8 and the HLA-DQ2α/DQ8β transdimer. *J. Immunol.* 187: 5123–5129.
16. Brochet, X., M. P. Lefranc, and V. Giudicelli. 2008. IMGT/V-QUEST: the highly customized and integrated system for IG and TR standardized V-J and V-D-J sequence analysis. *Nucleic Acids Res.* 36: W503–8.
17. Quigley, M. F., J. R. Almeida, D. A. Price, and D. C. Douek. 2011. Unbiased molecular analysis of T cell receptor expression using template-switch anchored RT-PCR. *Curr. Protoc. Immunol.* Chapter 10: Unit 10:33.
18. Price, D. A., J. M. Brenchley, L. E. Ruff, M. R. Betts, B. J. Hill, M. Roederer, R. A. Koup, S. A. Migueles, E. Gostick, L. Wooldridge, et al. 2005. Avidity for antigen shapes clonal dominance in CD8+ T cell populations specific for persistent DNA viruses. *J. Exp. Med.* 202: 1349–1361.
19. Boulter, J. M., M. Glick, P. T. Todorov, E. Baston, M. Sami, P. Rizkallah, and B. K. Jakobsen. 2003. Stable, soluble T-cell receptor molecules for crystallization and therapeutics. *Protein Eng.* 16: 707–711.
20. Garboczi, D. N., P. Ghosh, U. Utz, Q. R. Fan, W. E. Biddison, and D. C. Wiley. 1996. Structure of the complex between human T-cell receptor, viral peptide and HLA-A2. *Nature* 384: 134–141.
21. Henderson, K. N., H. H. Reid, N. A. Borg, S. E. Broughton, T. Huyton, R. P. Anderson, J. McCluskey, and J. Rossjohn. 2007. The production and crystallization of the human leukocyte antigen class II molecules HLA-DQ2 and HLA-DQ8 complexed with deamidated gliadin peptides implicated in coeliac disease. *Acta Crystallogr. Sect. F Struct. Biol. Cryst. Commun.* 63: 1021–1025.
22. McPhillips, T. M., S. E. McPhillips, H. J. Chiu, A. E. Cohen, A. M. Deacon, P. J. Ellis, E. Garman, A. Gonzalez, N. K. Sauter, R. P. Phizackerley, et al. 2002. Blu-Ice and the Distributed Control System: software for data acquisition and instrument control at macromolecular crystallography beamlines. *J. Synchrotron Radiat.* 9: 401–406.
23. Winn, M. D., C. C. Ballard, K. D. Cowtan, E. J. Dodson, P. Emsley, P. R. Evans, R. M. Keegan, E. B. Krissinel, A. G. Leslie, A. McCoy, et al. 2011. Overview of the CCP4 suite and current developments. *Acta Crystallogr. D Biol. Crystallogr.* 67: 235–242.
24. Storoni, L. C., A. J. McCoy, and R. J. Read. 2004. Likelihood-enhanced fast rotation functions. *Acta Crystallogr. D Biol. Crystallogr.* 60: 432–438.
25. Bridgeman, J. S., A. K. Sewell, J. J. Miles, D. A. Price, and D. K. Cole. 2012. Structural and biophysical determinants of αβ T-cell antigen recognition. *Immunology* 135: 9–18.
26. Rossjohn, J., S. Gras, J. J. Miles, S. J. Turner, D. I. Godfrey, and J. McCluskey. 2015. T cell antigen receptor recognition of antigen-presenting molecules. *Annu. Rev. Immunol.* 33: 169–200.
27. Davis, M. M., and P. J. Bjorkman. 1988. T-cell antigen receptor genes and T-cell recognition. *Nature* 334: 395–402.
28. Nikolich-Zugich, J., M. K. Slifka, and I. Messaoudi. 2004. The many important facets of T-cell repertoire diversity. *Nat. Rev. Immunol.* 4: 123–132.
29. Arstila, T. P., A. Casrouge, V. Baron, J. Even, J. Kanellopoulos, and P. Kourilsky. 1999. A direct estimate of the human alphabeta T cell receptor diversity. *Science* 286: 958–961.
30. Bodd, M., M. Ráki, E. Bergseng, J. Jahnsen, K. E. Lundin, and L. M. Sollid. 2013. Direct cloning and tetramer staining to measure the frequency of intestinal gluten-reactive T cells in celiac disease. *Eur. J. Immunol.* 43: 2605–2612.